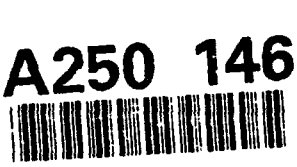

...USE ONLY (Leave blank)	2. REPORT DATE Feb. 28, 1992	3. REPORT TYPE AND DATES COVERED Final 16 Sep 91 - 31 Dec 91

4. TITLE AND SUBTITLE
Holographic Crosstalk and Signal-to-Noise Ratio in Orthogonal Data Storage

5. FUNDING NUMBERS
DAAL03-91-C-0050

6. AUTHOR(S)
George A. Rakuljic

7. PERFORMING ORGANIZATION NAME(S) AND ADDRESS(ES)
Accuwave Corp.
1653 - 19th Street
Santa Monica, CA 90404

8. PERFORMING ORGANIZATION REPORT NUMBER

9. SPONSORING/MONITORING AGENCY NAME(S) AND ADDRESS(ES)
U. S. Army Research Office
P. O. Box 12211
Research Triangle Park, NC 27709-2211

10. SPONSORING/MONITORING AGENCY REPORT NUMBER
ARO 29211.1-PHS

11. SUPPLEMENTARY NOTES
The view, opinions and/or findings contained in this report are those of the author(s) and should not be construed as an official Department of the Army position, policy, or decision, unless so designated by other documentation.

12a. DISTRIBUTION/AVAILABILITY STATEMENT
Approved for public release; distribution unlimited.

12b. DISTRIBUTION CODE

13. ABSTRACT *(Maximum 200 words)*

This final technical report summarizes our research performed under contract number DAAL03-91-C-0050. The holographic crosstalk and signal-to-noise ratio in orthogonal data storage were investigated by storing both plane holograms and high resolution holograms in a photorefractive crystal. These results were then used to predict the storage capacities of various photorefractive crystals using the orthogonal data storage technique.

14. SUBJECT TERMS Orthogonal data storage; Holographic crosstalk and signal-to-noise ratio			**15. NUMBER OF PAGES** 25 **16. PRICE CODE**
17. SECURITY CLASSIFICATION OF REPORT UNCLASSIFIED	**18. SECURITY CLASSIFICATION OF THIS PAGE** UNCLASSIFIED	**19. SECURITY CLASSIFICATION OF ABSTRACT** UNCLASSIFIED	**20. LIMITATION OF ABSTRACT** UL

Holographic Crosstalk and Signal-to-Noise Ratio in Orthogonal Data Storage

1.0. Introduction

Three dimensional optical data storage is a subject of considerable research interest today. Enormous data storage capacities are promised by such systems. Assuming diffraction-limited performance, storage of 10^{12} bits in a 1 cm^3 volume is predicted.[1] However, fast parallel access of the data or images stored in these large optical memories is not possible with all architectures. For example, those that rely on two-photon excitation are necessarily only bit by bit addressable.[2] Holographic techniques, on the other hand, offer both speed and capacity because of their inherent parallelism and large storage densities.

Unfortunately, previous demonstrations of volume holographic optical memories have resulted in data storage densities much less than the theoretical limit.[3-12] Although material difficulties significantly contribute to these shortcomings, a more fundamental problem existed with the angular multiplexing schemes used to holographically access the volume of the storage medium.[7-9] The scheme often used is one in which many two-dimensional patterns or images are sequentially recorded with successively angle-multiplexed reference waves. Holograms stored in this manner suffer from excessive crosstalk. This decreases the storage capacity of the recording medium since larger than expected angular separations are needed to adequately reduce the crosstalk. These difficulties arise from the inherent, inefficient "use" of K-space by the angular multiplexing method.

The orthogonal data storage concept[13-14] overcomes this problem in a basic fashion. The data are optically stored in a volume by recording many reflection holograms containing the information or images using counter-propagating reference waves and wavelength multiplexing. This technique permits the storage density of the medium to

approach the theoretical limit because of the lower crosstalk between wavelength channels due to the efficient spreading of the stored information throughout K-space as well as the physical volume. These points are shown in the following analysis.

2.0. K-space Analysis

The crosstalk and data storage properties of a volume holographic based optical memory can be studied by a K-space analysis. Any information-bearing image can be decomposed into an angular spectrum of plane waves. For high resolution images, the angular spread of these waves is essentially contained within a 45 degree half-angle cone. A hologram of an image stored in a volume is a result of the interference of each of these plane waves with the reference wave. As shown in Figure 1(a), the grating wavevectors of a hologram recorded by the orthogonal data storage method lie on the surface of a sphere of radius k centered on $(0,0,k)$.

In orthogonal data storage, wavelength multiplexing is used to store multiple images. Each stored image corresponds to a distinct wavelength and distinct surface along which the image grating wavevectors lie (see Figure 1(b)). The radius and center of curvature of the spheres are determined solely by the wavelengths used to store the data. The storage of multiple holograms results in a series of concentric "shells" in K-space as shown in Figure 2. The series of image grating wavevector surfaces are intentionally restricted to a spectral range from k to 2k to prevent scattering from any second order gratings that may be present.

The condition for low crosstalk between holograms is that each grating wavevector curve be sufficiently separated from that of another image. Consider Figs. 3 and 4 which show the relevant wavevectors for two stored holograms in the orthogonal data storage and angular multiplexing examples, respectively. In the case of orthogonal data storage, this separation is seen to be nearly uniform across the angular spread of the image wavevectors. In contrast, the separation varies strongly across the grating surfaces in the

angular multiplexing case. To limit the crosstalk, one must either limit the angular extent of each image surface, which is equivalent to limiting image resolution, or one must increase the overall angular separation between holograms, which limits the total number of stored holograms. Either method reduces storage capacity. On the other hand, with the orthogonal data storage technique, an increase in image detail does not increase the crosstalk between neighboring holograms. Therefore, higher density storage is possible with orthogonal data storage.

3.0. Sidelobe Suppression

A further reduction in the crosstalk between wavelength channels has been observed with the orthogonal data storage technique using photorefractive crystals. Figure 3 shows that the "information-independent" crosstalk that remains depends only on the spectral properties of a plane reflection hologram, and these are easily computed from theory.[15,16] However, recent experiments have shown that the observed crosstalk is much less than expected because of the self-induced sidelobe suppression that is seen in holograms stored in certain photorefractive crystals by this method.

These experimental studies of the noise and crosstalk properties of plane holograms involved storing a series of holograms at equal wavelength separations, but with the "middle" wavelength address hologram being left out. When this vacant position is illuminated by its corresponding wavelength radiation, there should be zero readout. Any output from this "missing" hologram is the noise and crosstalk contributions from the other holograms.

Figure 5 shows the setup that was used to write and characterize the holograms using orthogonal data storage. Simple plane waves were used as the object beam by removing the transparency T. The system consists of a high resolution, scanning dye laser integrated with a highly accurate wavemeter all under computer control. A 2 mm thick lithium niobate crystal with the c-axis perpendicular to the polished optical faces was

used as the storage medium. The writing beams were oriented in a counterpropagating geometry for true orthogonal storage, with the orthogonal dimensions being x, y, and λ.

Figure 6 shows the theoretical response of a single, 2 mm thick plane hologram. A wavelength separation of > 40 Å is required to obtain sidelobe levels of < -50 dB, for example. Compare this to the actual measured results shown in Figure 7, where only a 10 Å separation suffices for the same -50 dB sidelobe level. This naturally occurring sidelobe reduction is routinely observed with the orthogonal data storage technique. This side lobe suppression cannot be fully attributed to apodization of the modulation index caused by the absorption in the crystal, for example; further investigation is needed to understand this phenomenon.

Figures 8 and 9 show further results obtained with 7 and 20 plane holograms, respectively. At a separation of 10 Å, the zero level in the middle unrecorded hologram was -45 to -50 dB for the 7 hologram case, while a figure of -35 to -40 dB was observed for the 20 hologram example. These results are better than what has been previously published using angular multiplexing (see Ref. 17, for example), especially considering that electrical SNR figures in the detection circuit are often presented ($20\log(I_S/I_N) = 20\log(P_S/P_N)$), rather than the optical SNR ($10\log(P_S/P_N)$), as is done here.

4.0. Orthogonal Data Storage Experiments

The holographic noise and crosstalk in orthogonal data storage were investigated by recording a number of different, high resolution holograms of the integrated circuit mask shown in Figure 10. This mask, consisting of 5 μm lines, was used as the transparency T in Figure 5.

Figures 11 to 15 summarize the experimental results using the same 2 mm thick photorefractive crystal. Except for Figure 15, where the wavelength separation was 5 Å to keep the wavelength span within the optimal range of the dye laser, the other holograms were written 10 Å apart. The major sources of noise in these experiments

unwanted surface scattering and reflections of the reference beam off the crystal during readout. Additional difficulties with beam coupling between the original beams and the multiple Fresnel reflections in the crystal during the writing phase were encountered. This decreased image fidelity. To minimize this effect the exposure times were reduced at the expense of signal strength, thus preserving the fidelity of the stored holograms.

Table 1 summarizes the SNR values measured for the holograms in Figs. 11 to 15. As the number of holograms was increased, the roll off in SNR was mainly due to decreasing diffraction efficiencies, and not from any real increase in holographic noise or crosstalk. The SNR measurements in these experiments were limited by surface reflections and scattering off the crystal and the numbers given here represent a lower bound since the holographic noise and crosstalk were not strong enough to be detected. More accurate measurements of the holographic noise and crosstalk require a photorefractive crystal with a very high quality polish and efficient antireflection coating.

5.0. SNR vs. Number of Holograms

The data in Table 1 can be used as a basis for predicting the storage capacity that can be obtained with orthogonal data storage and thicker crystals or crystals with higher dopant concentrations to increase the coupling constant. Consider the signal-to-noise ratio of the diffracted signal from a hologram, which is given by

$$\mathrm{SNR} = 10 \log\left(\frac{P_S}{P_N}\right)$$

The noise level P_N was essentially constant in the above experiments, so the decrease in SNR with increasing hologram number is attributed to the decrease in signal only. For counterpropagating gratings, the signal is given by the relation

$$P_S = R = \tanh^2(\kappa l)$$

where R is the reflectivity of the hologram, κ is the coupling constant, and l is the thickness of the crystal. Note that as the crystal thickness is increased, κl also increases.

The coupling constant depends on dopant level and is proportional to the space charge field $E_{sc} \approx E_{PV}$, typically, in lithium niobate. The photovoltaic field E_{PV}, however, is proportional to the dopant concentration, assuming constant reduction ratios. Therefore, the coupling constant also scales linearly with the dopant concentration, so that a factor of 2 increase in the dopant concentration should also double the coupling constant.

Increasing κl leads to stronger holograms and larger signal-to-noise ratios or increased storage capacity for the same SNR. The scaling factor for signal strength per hologram vs. the signal strength for one hologram can be determined by examining the sum of a large number of sine waves with different periods, and then comparing the total to the magnitude of a single sine wave at saturation. Two extremes result. The correlated holograms case represents the worst case for multiple storage since every hologram will coherently overlap at various points throughout the crystal. Therefore, the κl of each hologram decreases as 1/N of the single hologram case since the charge carriers must equally distribute themselves at the maxima of all the gratings. The best case is for completely uncorrelatated holograms, where the phases are random so the charge carriers are distributed uniformly over the average value of the sinusoidal gratings. In this case, the scale factor is $1/\sqrt{N}$, allowing storage of more holograms with the same signal to noise ratio. As an example, a 10-fold increase in κl (which can be realized by increasing thickness from 0.2 to 1.0 cm and doubling the dopant concentration) should theoretically allow the storage of 10 to 100 times the current capacity with the same SNR, depending on the degree of correlation among the holograms. The expected storage capacities are summarized in Table 2 for both cases.

6.0. Summary

In summary, the noise and crosstalk properties of holograms were studied by recording a number of wavelength multiplexed holograms, both plane wave and image bearing, in $LiNbO_3$ using the orthogonal data storage technique. The spillover diffraction of recorded holograms into vacant wavelength sites indicated the degree of noise and crosstalk in the hologram. However, the high surface reflection and scattering effects in the crystals were significantly larger than the holographic noise or crosstalk. The bandwidth of a single, counterpropagating reflection mode hologram recorded in a 2 mm thick crystal was measured to be less than 10 Å for a -50 dB crosstalk level, which is 4 times less than the expected theoretical value. This is partially attributed to apodization of the index grating due to bulk absorption in the material. Further investigation is warranted in the areas of noise studies and sidelobe suppression with very high quality, anti-reflection coated crystals and the orthogonal data storage technique.

References

1. P.J. van Heerden, Appl. Opt. **2**, 393 (1963).
2. S. Hunter, F. Kiamilev, S. Esener, D.A. Parthenopoulos, and P.M. Rentzepis, Appl. Opt. **29**, 2058 (1990).
3. P.D. Henshaw, S.A. Lis, and N.R. Guivens, Jr., "Compact 4-D Optical Neural Network Architecture," Final Report, Contract No. F49620-89-C-0120, April 1990.
4. L. Hesselink and S. Redfield, Opt. Lett. **13**, 877 (1988).
5. L. Solymar and D.J. Cooke, Volume Holography and Volume Gratings (Academic Press, London, 1981).
6. W.J. Burke, P. Sheng, and H.A. Weakliem, "Intrinsic Noise Sources in Volume Holography," Final Report, Contract No. N00014-75-C-0590, December 1975.
7. B.D. Guenther, Army Research Office, private communication.
8. T. Jannson, Optica Acta **27**, 1335 (1980).
9. K. Blotekjaer, Appl. Opt. **18**, 57 (1979).
10. W.J. Burke, "Signal/Noise Ratio of Holographic Images," Final Report, Contract No. N00019-75-M-0494, October 1975.
11. A.M. Glass, Opt. Eng. **17**, 470 (1978).
12. P. Gunter, Phys. Reports **93**, 199 (1982).
13. G.A. Rakuljic, V. Leyva, and A. Yariv, "Volume Holography using the Orthogonal Data Storage Approach," paper FU-7, ,OSA Annual Meeting, San Jose CA, 1991.
14. A. Yariv, G.A. Rakuljic, and V. Leyva, "High Resolution Volume Holography using Orthogonal Data Storage," paper MD-3, OSA Topical Meeting on Photorefractive Materials, Effects, and Devices, Beverly MA, 1991.
15. H. Kogelnik, Bell Syst. Tech. J. **48**, 2909 (1969).
16. A. Yariv, Quantum Electronics (Wiley, New York, ed. 2, 1975).
17. W.J. Burke and P. Seng, J. Appl. Phys. **48**, 481 (1977).

ORTHOGONAL DATA STORAGE

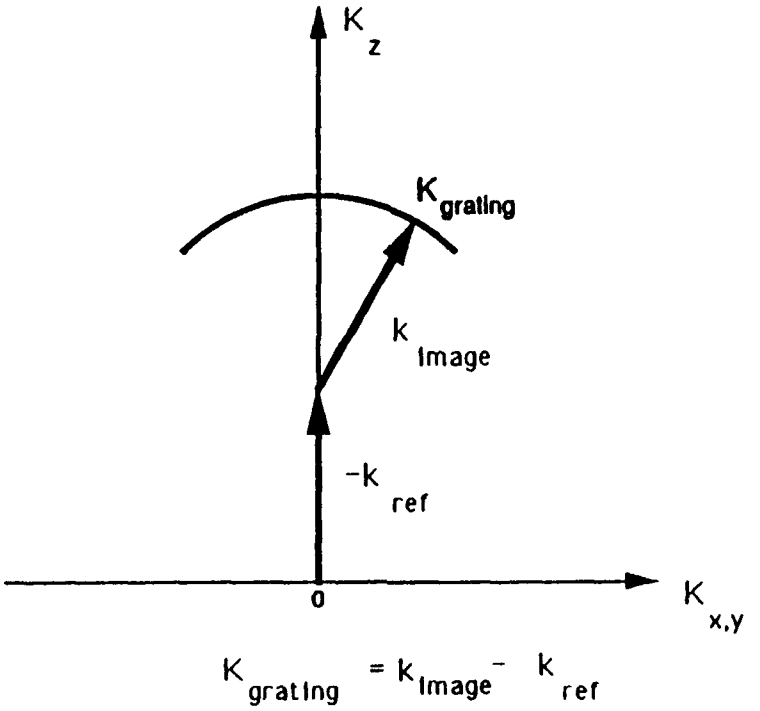

(a) Counter propagating, reflection mode geometry

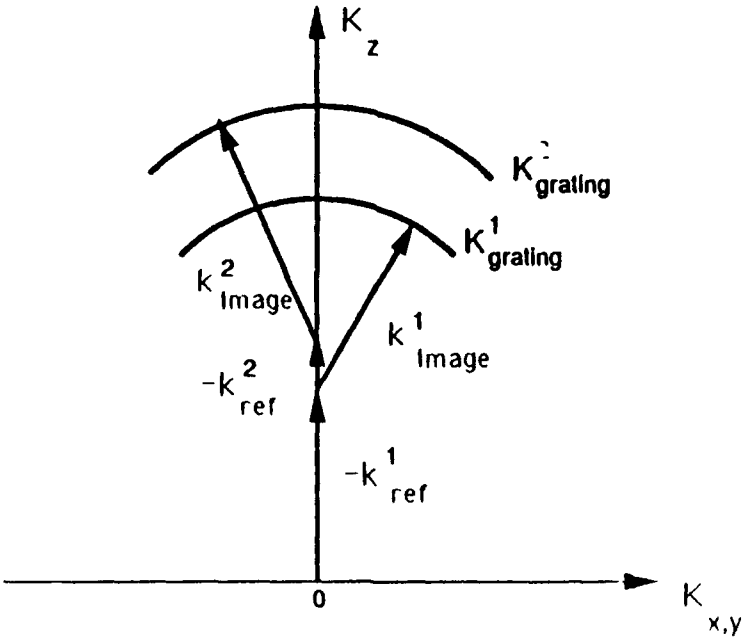

(b) Wavelength multiplexed, multiple image storage

Figure 1

STORAGE CAPACITY- ORTHOGONAL DATA STORAGE

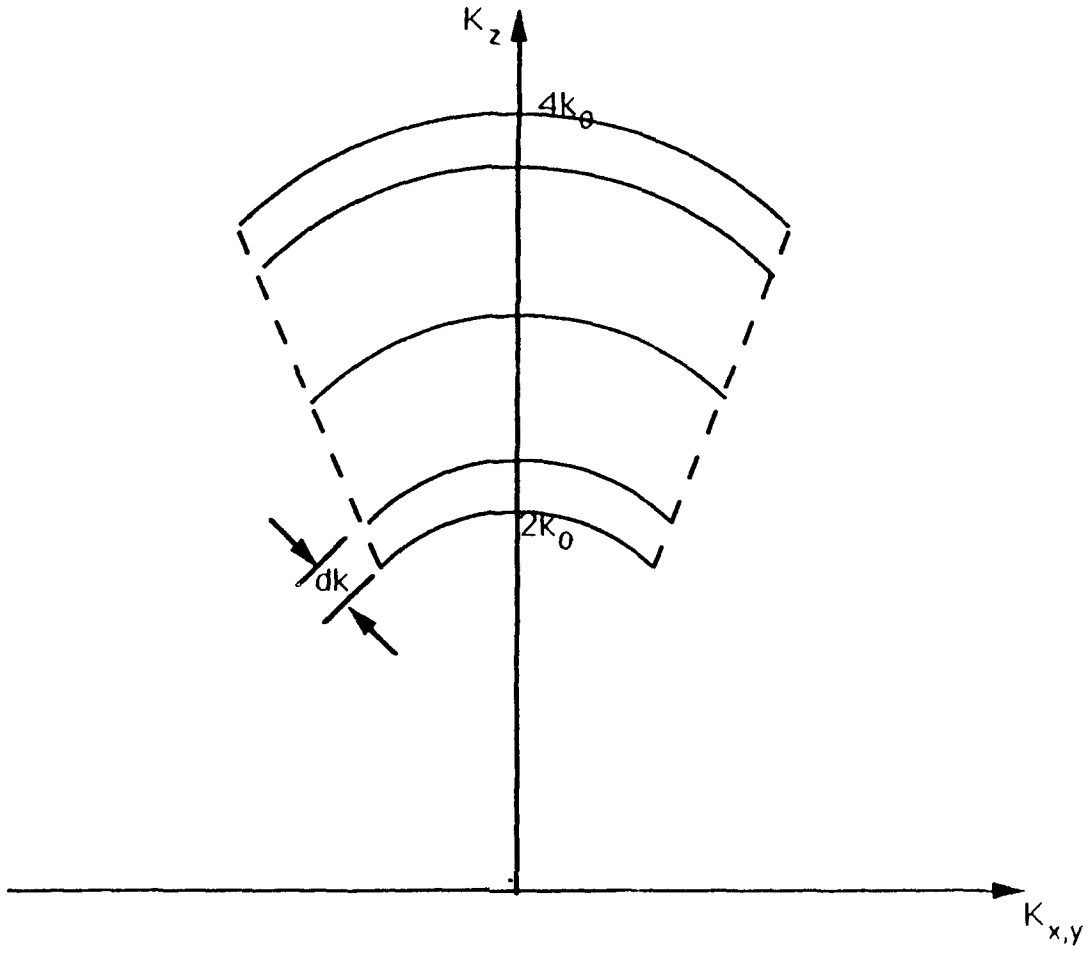

* Grating wavevectors lie on spherical shell

* multiplexed images form series of shells of curvature k_0 to $2k_0$

* Shells sweep out volume in K- space $V_K = \frac{7\pi}{3}(2-\sqrt{2})\,k_o^3$

* To prevent crosstalk grating wavevectors must be seperated by $dK_i = 2\pi/L_i$

*Storage capacity=# of independent gratings or bits

$$= \frac{V_K}{(dK)^3}$$

$$= \frac{7\pi}{3}(2-\sqrt{2})\,n^3\,\frac{\text{volume}}{\lambda_0^3}$$

Figure 2

IMAGE CROSSTALK USING ORTHOGONAL DATA STORAGE

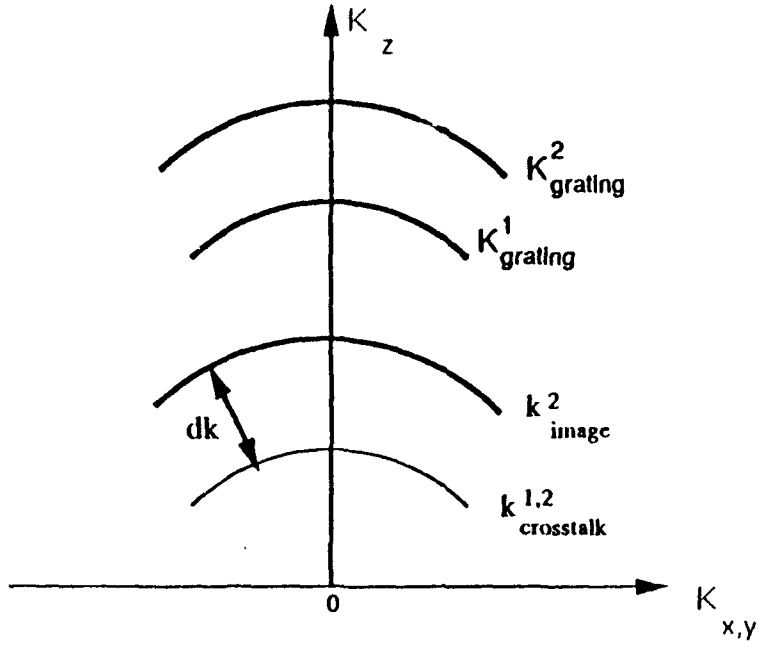

Two image gratings $K^2_{grating}$ and $K^1_{grating}$ are stored in the crystal

Readout is with k^2_{ref}

Get:

$k^2_{image} = K^2_{grating} + k^2_{ref}$ Reconstructed image

$k^{1,2}_{crosstalk} = K^1_{grating} + k^2_{ref}$ Noise from grating 1

Seperation dk must be sufficiently large to minimize image crosstalk

Note: seperation dk is virtually independent of information content in images

This allows for the efficient "packing" of images in k-space.

Hence, theoretical data storage limit of volume holography can be approached.

Figure 3

IMAGE CROSSTALK USING ANGULAR MULTIPLEXING

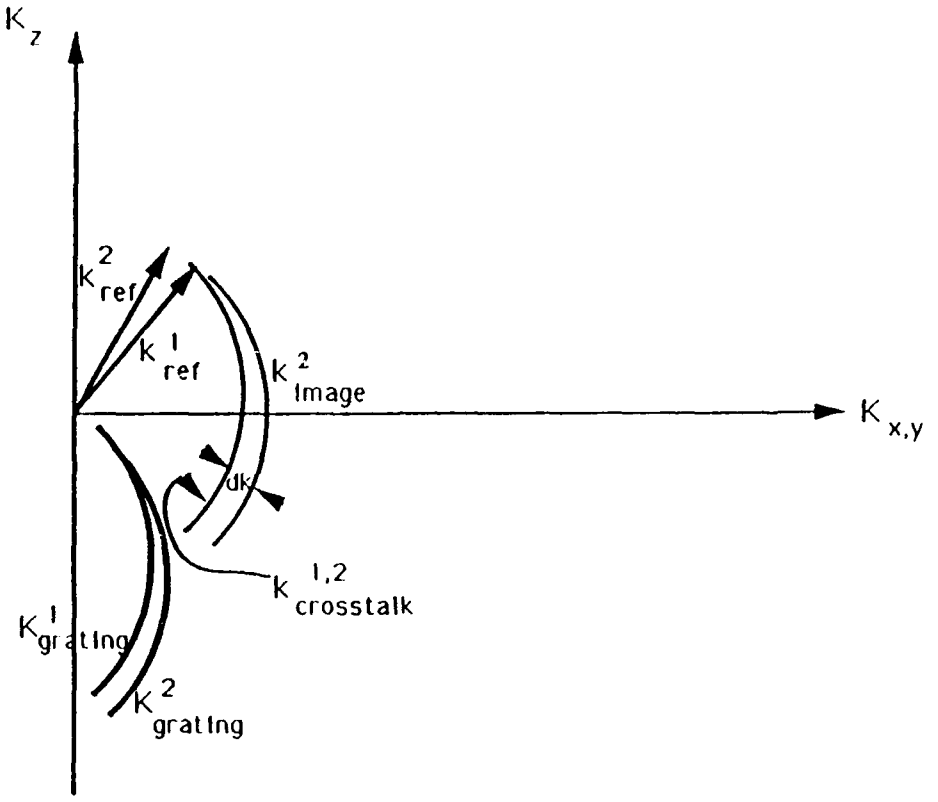

Two image gratings stored in crystal $K^1_{grating}$ and $K^2_{grating}$

Readout is with k^2_{ref}

Get: $k^2_{Image} = K^2_{grating} + k^2_{ref}$ Reconstructed image

$k^{1,2}_{crosstalk} = K^1_{grating} + k^2_{ref}$ Noise grating 1

dk must be sufficiently large to minimize crosstalk

Must limit information content per image (k spread) to keep dk sufficiently large

Figure 4

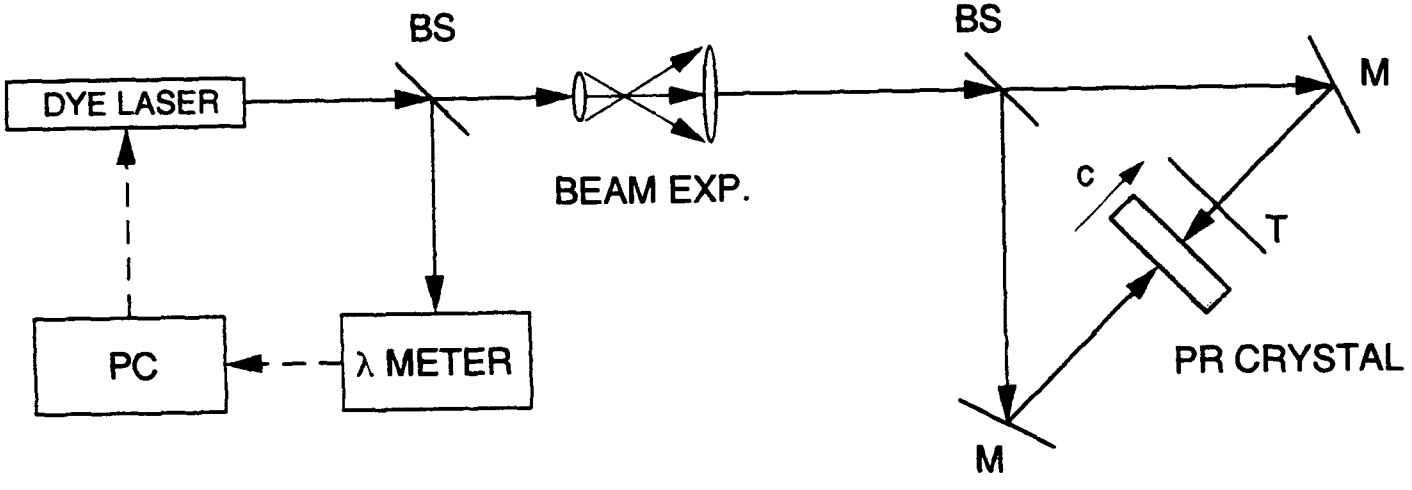

Figure 5: Experimental set-up for holographic recording using orthogonal data storage.

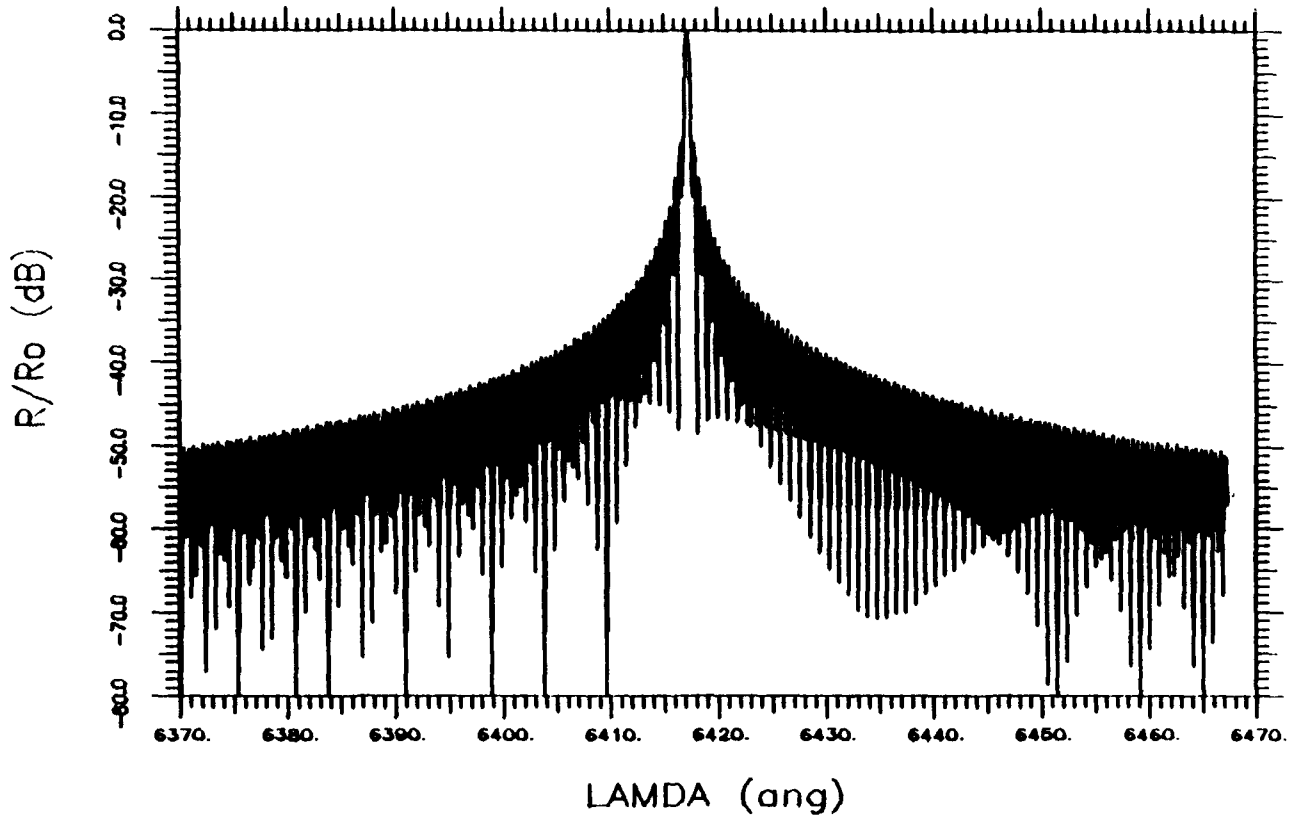

Figure 6: Theoretical response of a 2mm thick, unapodized holographic grating.

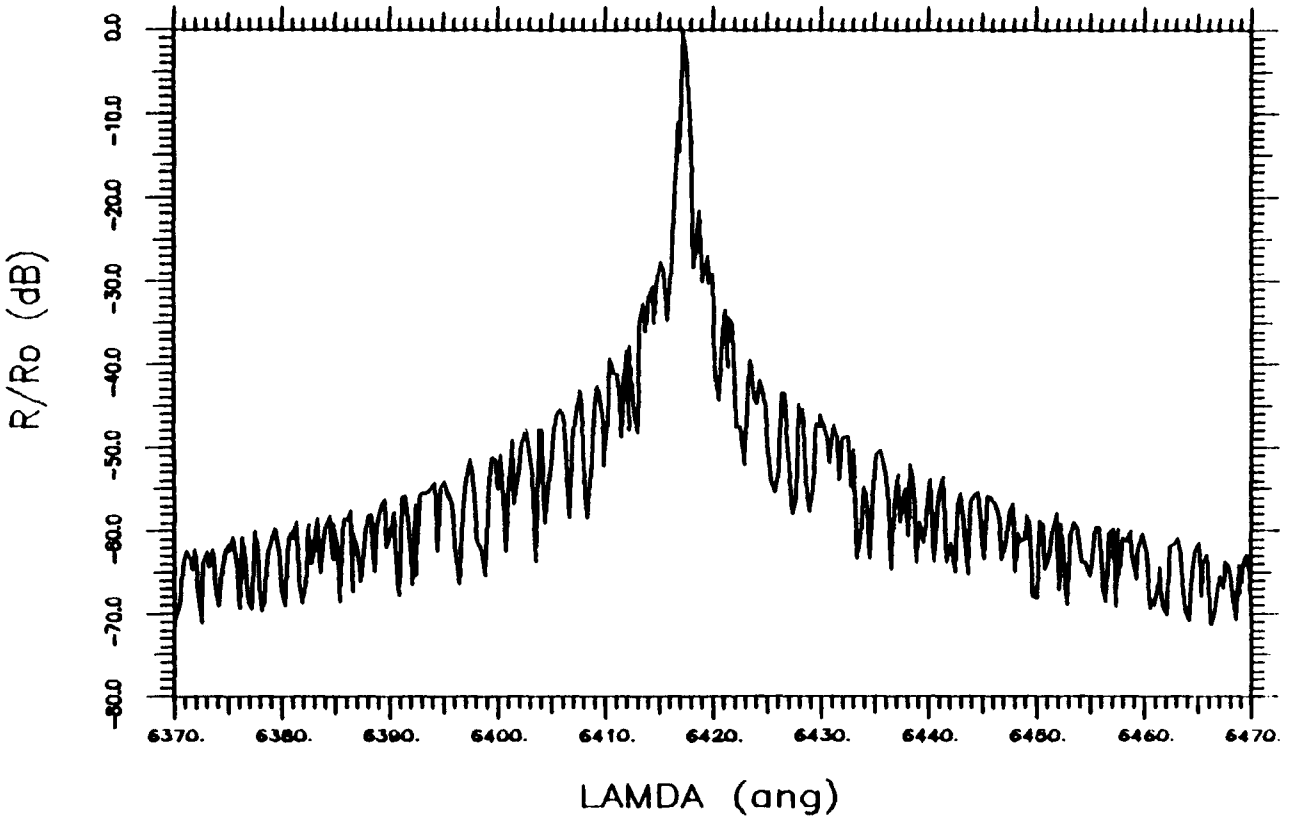

Figure 7: Actual response of a 2mm thick holographic grating recorded by the orthogonal data storage technique.

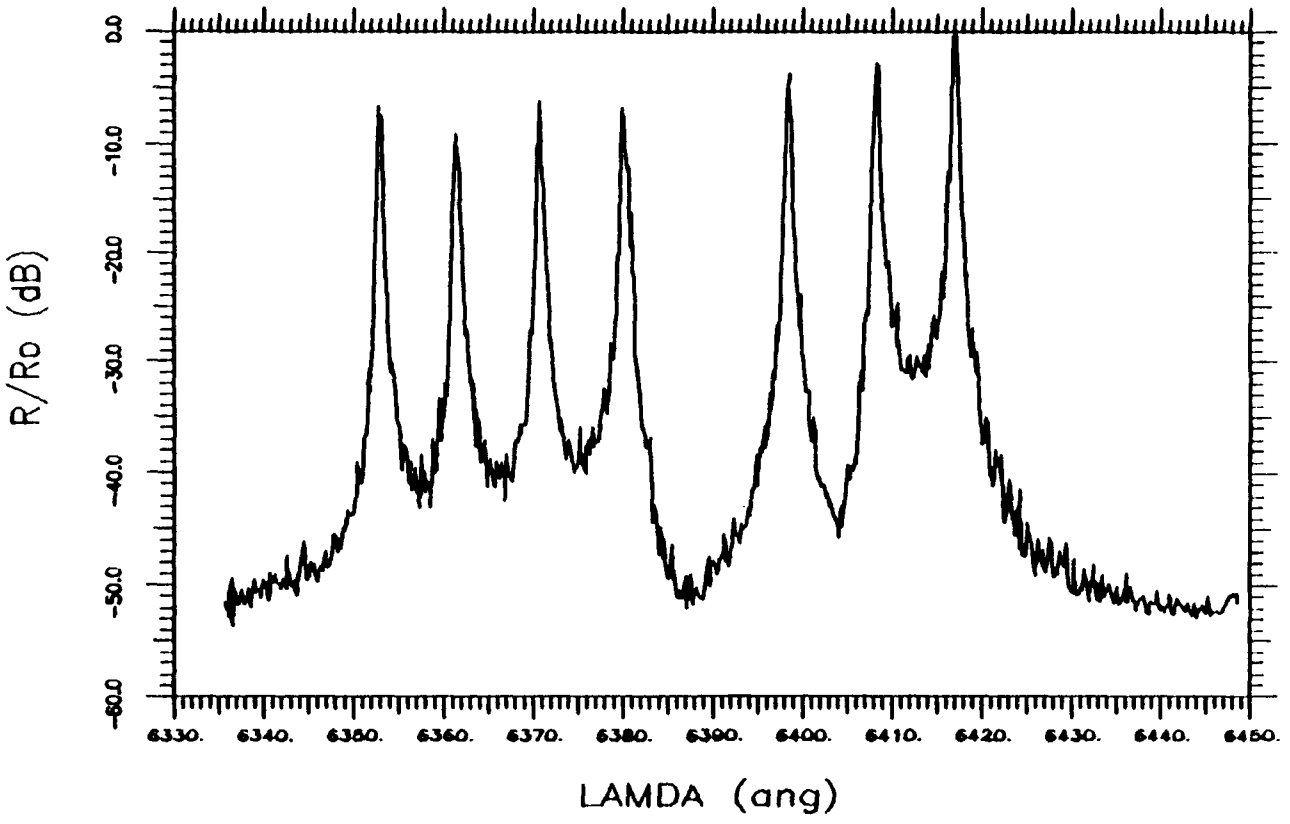

Figure 8: Actual response of 7, 2mm thick holographic gratings recorded by the orthogonal data storage technique.

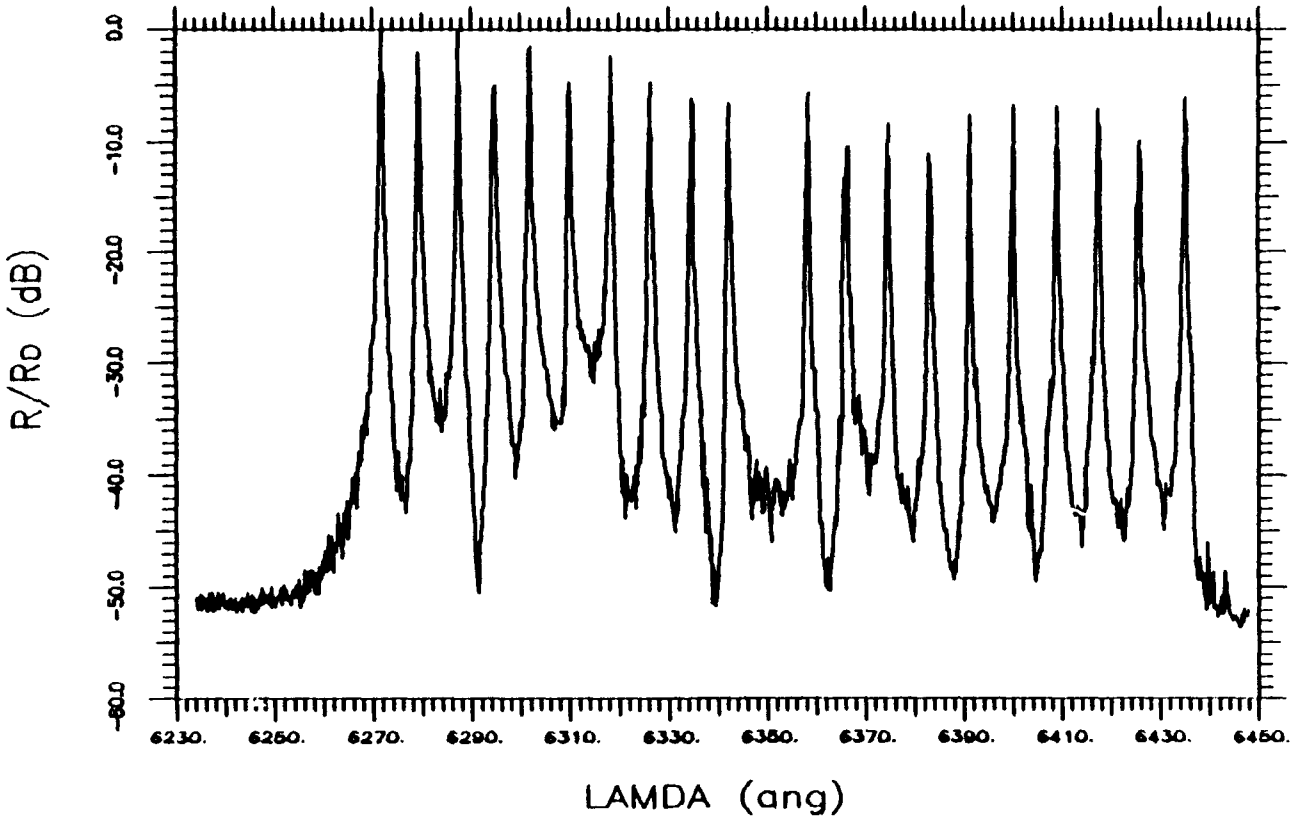

Figure 9: Actual response of 20, 2mm thick holographic gratings recorded by the orthogonal data storage technique.

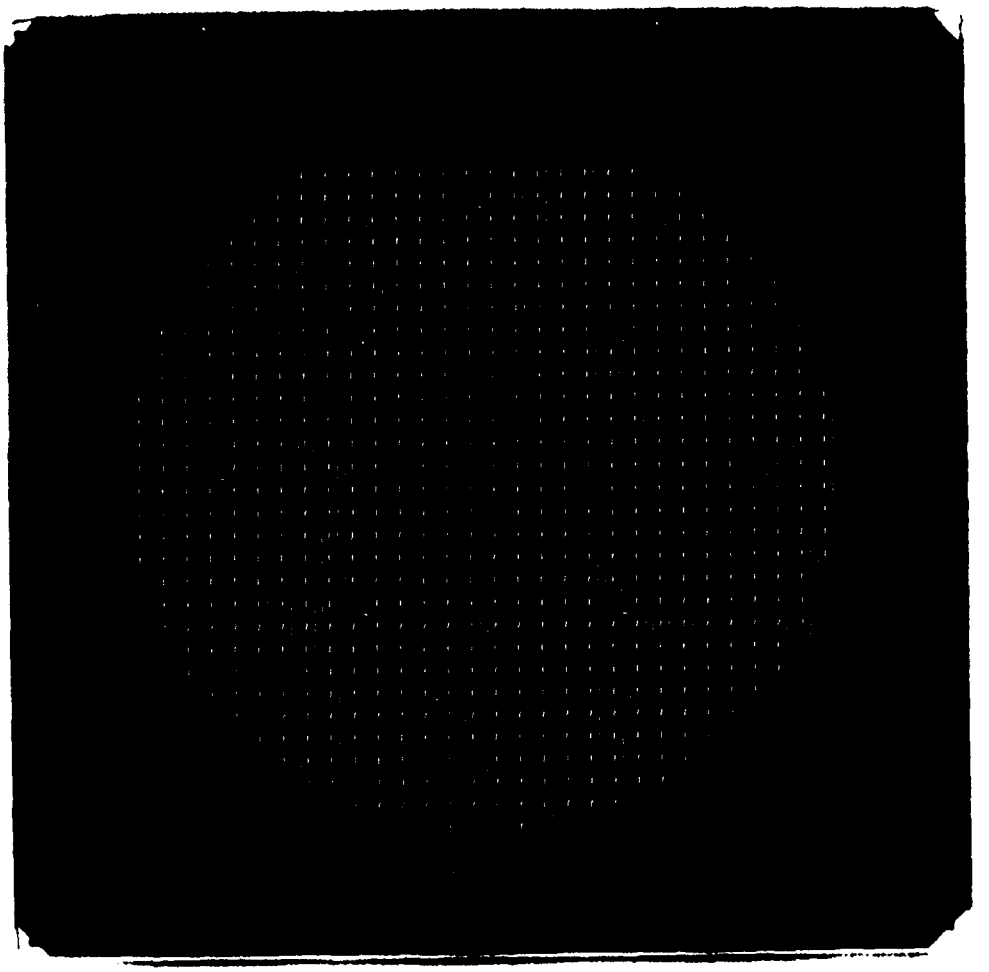

Figure 10: Transparency used in the holographic storage experiments. The smallest features are less than 5 microns in size.

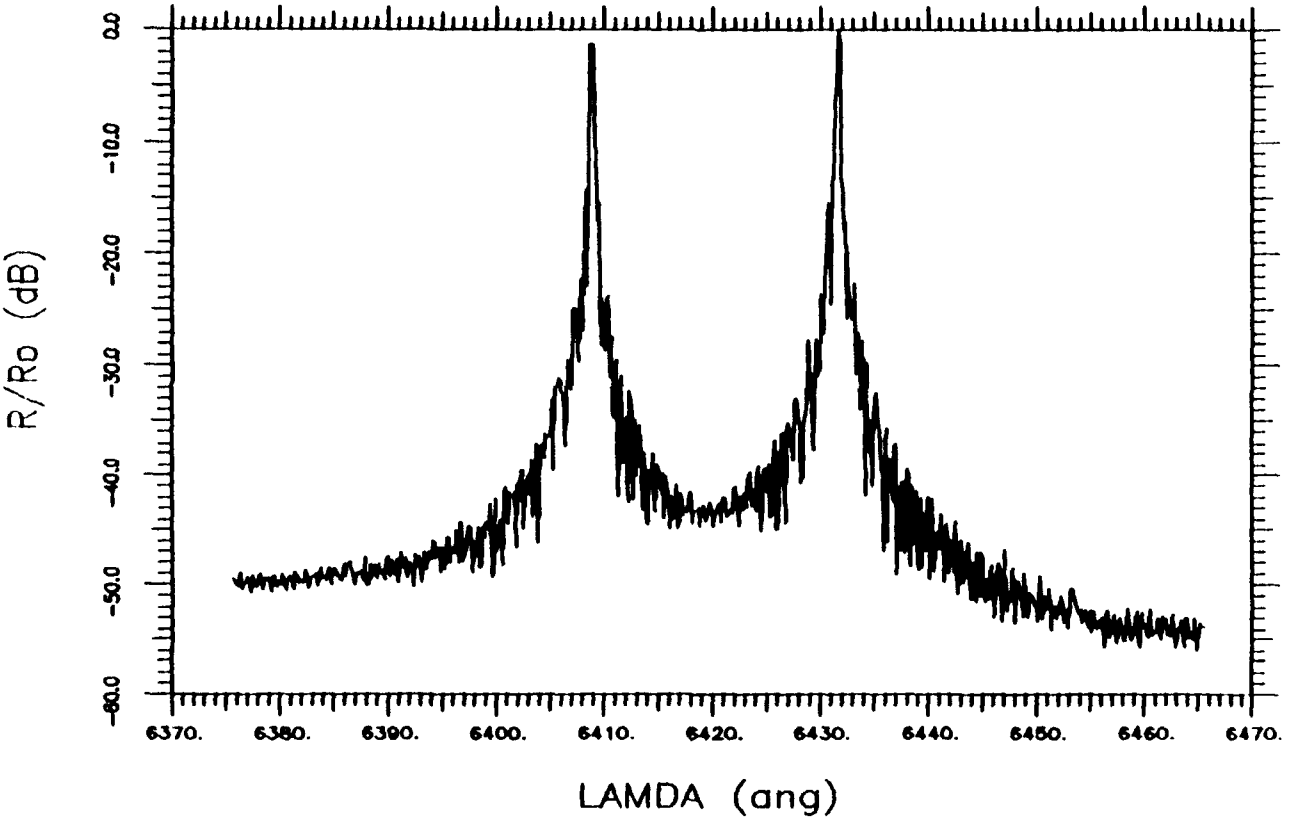

Figure 11: Actual response of 2 different high resolution images stored by the orthogonal data storage technique.

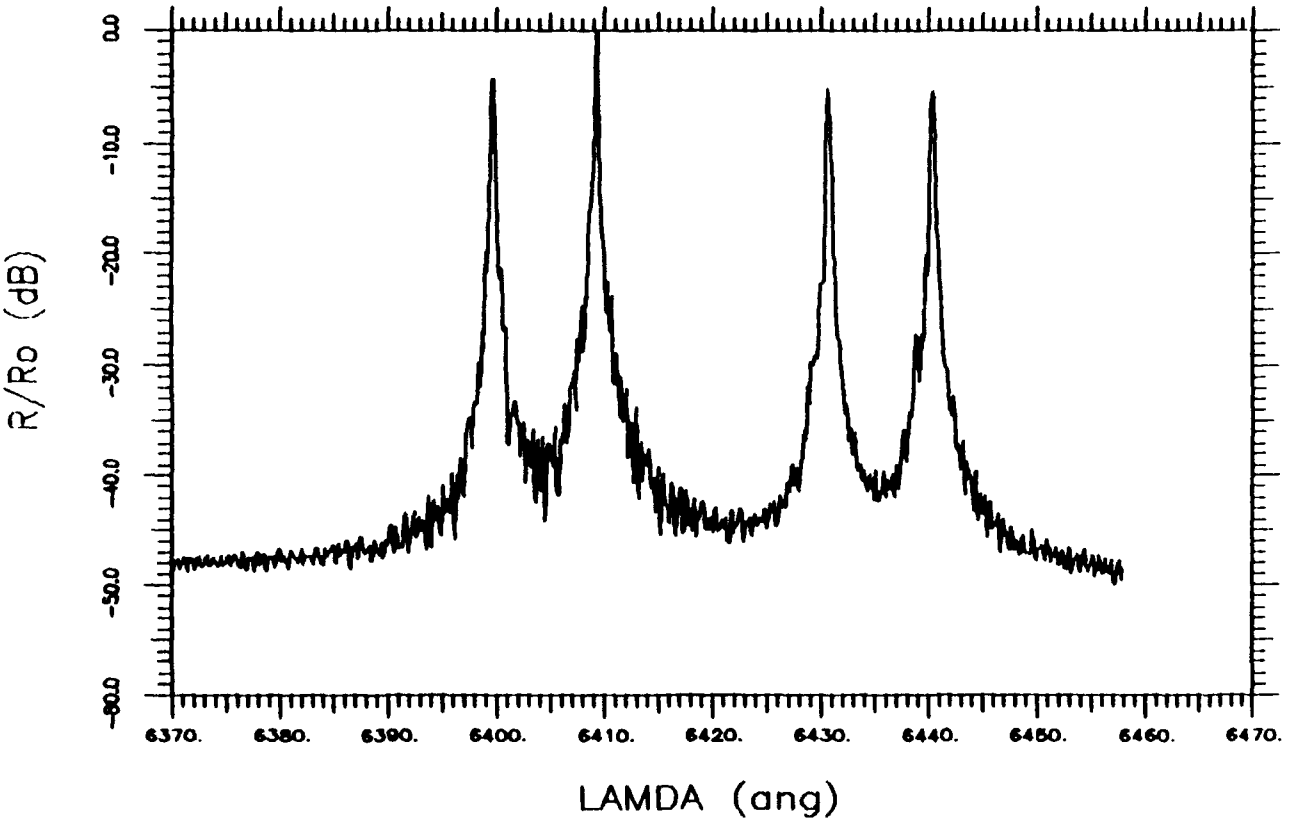

Figure 12: Actual response of 4 different high resolution images stored by the orthogonal data storage technique.

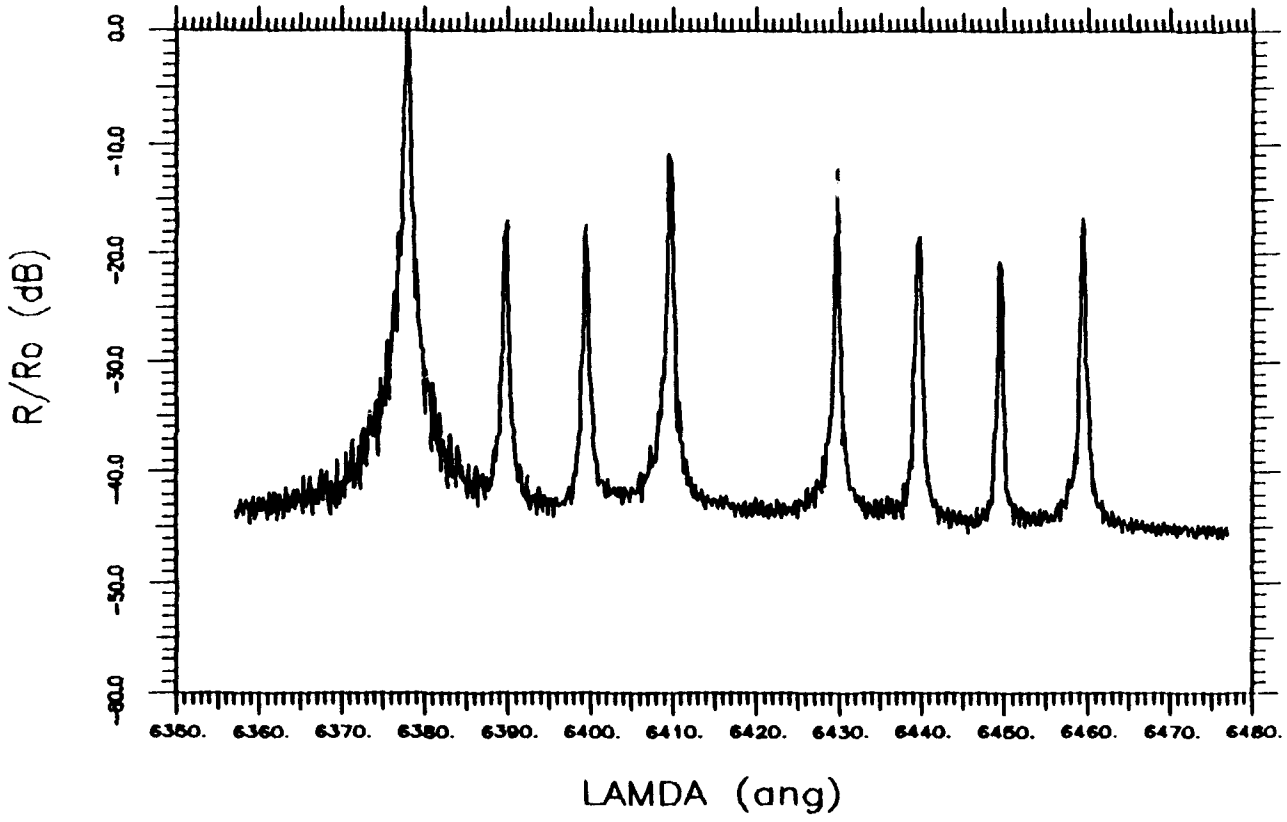

Figure 13: Actual response of 8 different high resolution images stored by the orthogonal data storage technique.

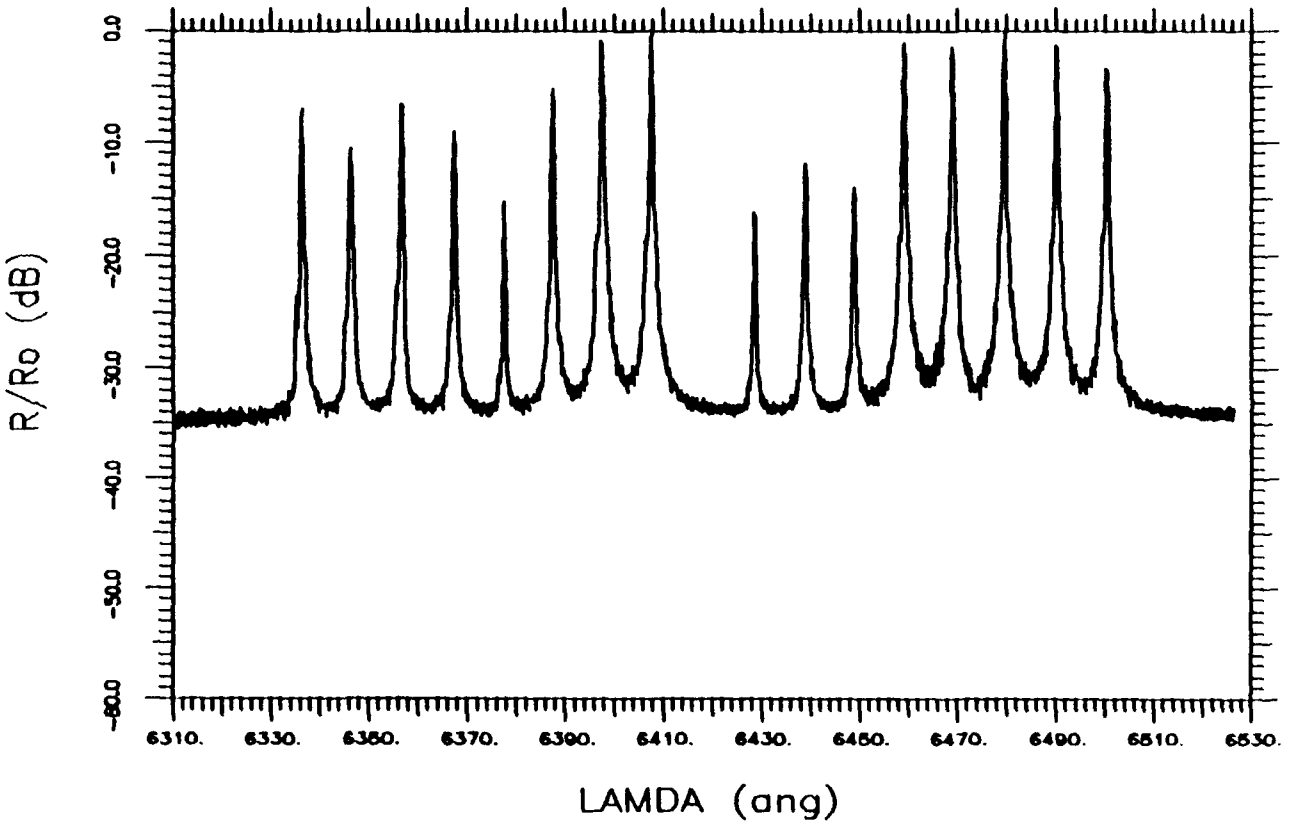

Figure 14: Actual response of 16 different high resolution images stored by the orthogonal data storage technique.

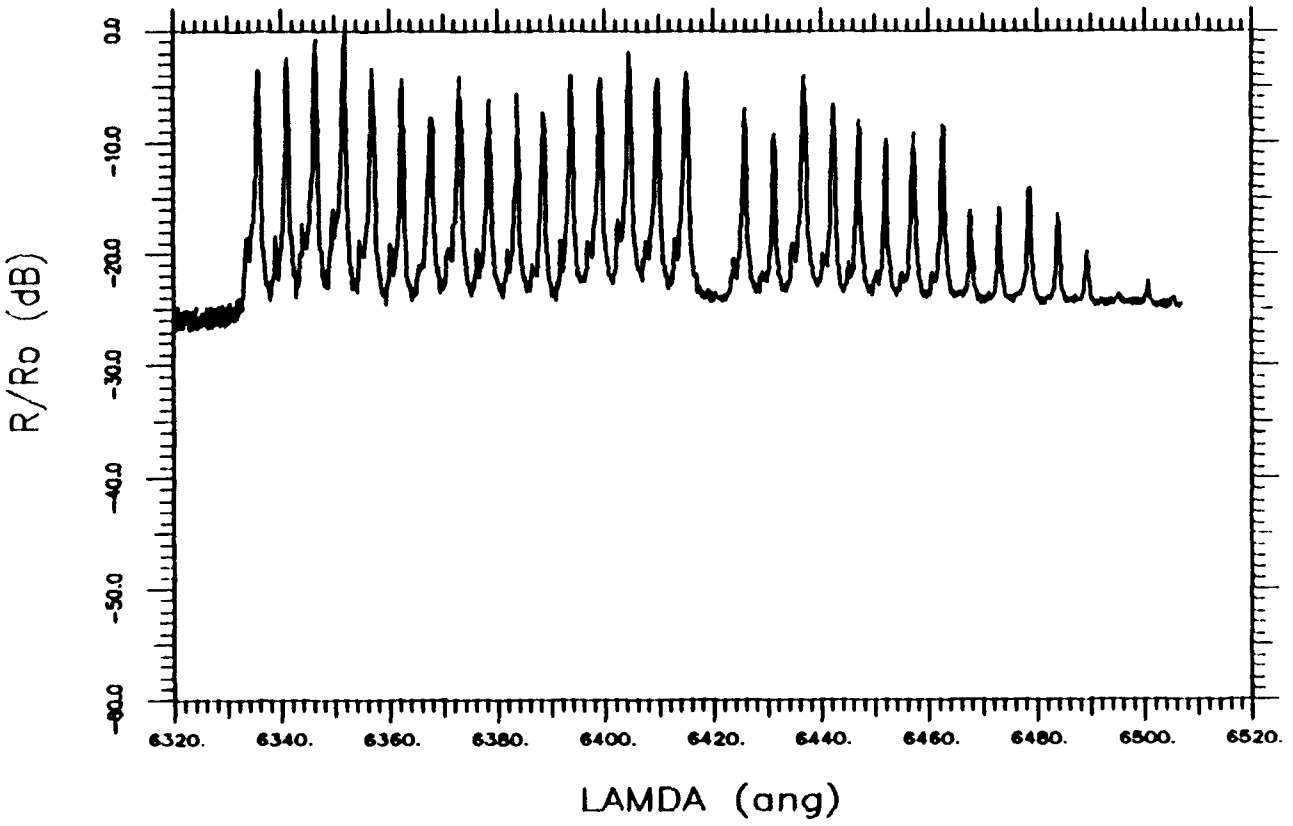

Figure 15: Actual response of 32 different high resolution holograms stored by the orthogonal data storage technique.

Sample thickness-2mm

No. of Holograms (10A channel seperation)	2	4	8	16	32*
Signal to Noise (dB) ($SNR=10\log(P_S/P_N)$)	44	44	43	33	24

* channel seperation- 5A

Note:SNR limited by surface reflections/scattering

Table 1: Summary of experimental results

SNR vs. Number of Holograms

SNR (dB)	1x dopant l = 0.2 cm	1x dopant l = 1 cm (Predicted)		2x dopant l = 1 cm (Predicted)	
		1/N rolloff	$1/\sqrt{N}$ rolloff	1/N rolloff	$1/\sqrt{N}$ rolloff
44	2	10	50	20	200
44	4	20	100	40	400
43	8	40	200	80	800
33	16	80	400	160	1,600
24	32	160	800	320	3,200

Table 2. Signal-to-noise ratio vs. number of high-definition holograms recorded in a photorefractive lithium niobate crystal using orthogonal data storage.